



## Temperature Effect on Creep and Fracture Behaviors of Nano-SiO<sub>2</sub>-composite and AlSi12Cu3Ni2MgFe Aluminum Alloy

M. Azadi\*, H. Aroo

Faculty of Mechanical Engineering, Semnan University, Semnan, Iran

### PAPER INFO

#### Paper history:

Received 21 February 2020

Received in revised form 26 March 2020

Accepted 07 June 2020

#### Keywords:

Creep Property

Piston Aluminum Alloy

Aluminum Alloy Matrix Nano-composite

Temperature Effect

Fracture Behavior

### ABSTRACT

In the presented article, the temperature effect was studied on creep properties and fracture behaviors of AlSi12Cu3Ni2MgFe aluminum-silicon alloys, unreinforced and reinforced with SiO<sub>2</sub> nano-particles. For such objective, standard specimens were fabricated by gravity casting and stir-casting methods, for aluminum alloys and nano-composites, respectively. Then, force-controlled creep testing was performed on standard specimens at 250, 275 and 300°C, under 100 MPa. Then, to find failure mechanisms, the fracture surface of test samples was also analyzed by the field emission scanning electron microscopy. Experimental results depicted the temperature changed creep behaviors of both materials, effectively. Moreover, a significant improvement in creep properties was observed by reinforcing the aluminum matrix with nano-particles, besides a heat treatment process. Such an increase in the creep lifetime was higher at 300°C. In addition, the fracture surface investigation of both materials implied the same brittle behavior, with quasi-cleavage marks. The failure location changed from inside the intermetallic phase into boundaries of the intermetallic phase in the nano-composite.

doi: 10.5829/ije.2020.33.08b.16

## 1. INTRODUCTION

Nowadays, aluminum alloys have been vastly utilized in engine and automotive industries, due to advantages such as good casting behavior, low density, proper wear resistance and moderate thermal behavior [1-3]. In order to improve these characteristics, especially at higher temperatures for engine piston applications, the addition of the nickel element to the alloy and the heat treatment process could be used. As an innovative approach, ceramic-reinforced aluminum matrix composites have been developed by adding nano-particles.

According to the operation condition of engine pistons, high-temperature behaviors of the material should be investigated, such as the creep lifetime and the stress relaxation. In this field of study, different articles were presented for aluminum-silicon alloys. Although investigations about creep properties of metal matrix composites are still rare. In following paragraphs, a literature review could be seen for aluminum alloys, not

in details. Since the main topic is to highlight the nano-composite.

Ishikawa et al. [4] studied creep behaviors of highly pure aluminum at lower temperatures. They showed that the creep rate depended upon the applied stress and the cyclic stress had an effect on the creep lifetime. Jenabali Jahromi [5] presented creep behaviors of the spray-cast heat-treatable AlZnMgCuZr aluminum alloy. Their creep rate results at 120°C indicated a much lower rate of the alloy, compared to the ingot-cast 7075 aluminum alloy. Ishikawa and Kobayashi [6] found that the minimum strain rate was seen instead of the steady state condition in creep and rupture behaviors of the A5083 aluminum-magnesium alloy. Dobes and Milicka [7] studied creep behaviors of Al-5.5wt.%Mg and Al-13.7wt.%Zn aluminum solid solutions, at 300 to 500°C. Srivastava et al. [8] investigated the low-stress creep behavior of the 7075 high strength aluminum alloy, at 350-410°C to find the stress exponent. Lin et al. [9] demonstrated that the stress had a significant effect on the whole creep

\*Corresponding Author Institutional Email: [m\\_azadi@semnan.ac.ir](mailto:m_azadi@semnan.ac.ir)  
(M. Azadi)

deformation process at 250°C for the pure copper and at 150°C for the aluminum alloy.

Requena and Degischer [10] presented creep behaviors of unreinforced and short fiber reinforced AlSi12Cu3Ni2MgFe aluminum alloys at 300°C. They found that 15 vol.% of the reinforcement was the highest creep resistant, while 20 vol.% had lower creep resistant than 10 and 15 vol.%, due to its higher defect density and larger interface area. Couteau and Dunand [11] studied the creep behavior of aluminum syntactic foams at 500°C and showed that the minimum strain rate varied with the stress, by changing the stress exponent. Kandare et al. [12] modeled creep-based lifetime prediction of aluminum in fire. The model was validated by fire structural tests, performed on a non-age-hardening 5083 H116 aluminum alloy. Li et al. [13] presented modeling of high-temperature creep behaviors of 7075 and 2124 aluminum alloys by continuum damage mechanics, with a good agreement. Maximov et al. [14] modeled strain hardening and creep behaviors of the 2024-T3 aluminum alloy at different temperatures. The constitutive model authenticity was proved experimentally, besides finite element simulations.

Zhan et al. [15] studied effects of process parameters on mechanical properties and the microstructure of creep-aged 2124 aluminum alloys. Their results implied that the creep strain and the creep rate increased by increasing the ageing time, the temperature and the stress. Fernandez-Gutierrez and Requena [16] investigated the effect of the spheroidization heat treatment on the creep resistance of a cast AlSi12CuMgNi aluminum alloy. They indicated that the highest creep resistance gradually decreased by increasing the solution treatment time, due to the loss of the load bearing capability of rigid phases. Zhang et al. [17] evaluated asymmetric tensile and compressive creep behaviors in the ZL109 aluminum alloy. They found that at high temperatures or high stress levels, the ratio between tensile and compressive creep rates was as large as 10. Spence and Makhlof [18] indicated that residual compressive stresses on the machined surface caused the material to creep and the creep rate increased by increasing the temperature in 4032-O and 6061-T6 aluminum alloys. Yang et al. [19] simulated the AA2524 aluminum alloy in creep age forming at temperatures of 180-200°C.

Lie et al. [20] showed that due to fine transgranular precipitates, the creep-aged 7050 aluminum alloy with initial tempers of the solution and the re-solution exhibited higher mechanical properties than that of the retrogression with coarse transgranular precipitates. Erdeniz et al. [21] studied the effect of vanadium micro-alloying on microstructural and creep behaviors of Al-Er-Sc-Zr-Si aluminum alloys, with and without L1<sub>2</sub>-ordered coherent Al<sub>3</sub>(Er,Sc,Zr) nano-scale precipitates. Xu et al. [22] found that the creep strain magnitude of the 2524 aluminum alloy greatly increased with increasing the pre-

strain due to the precipitation process, reducing the average size of Al<sub>2</sub>CuMg phases. Li et al. [23] developed a unified constitutive model for creep-ageing of the AA2050-T34 Al-Cu-Li alloy. Yang et al. [24] investigated the effect of the pre-deformation on creep age forming of the 2219 aluminum alloy. Their results indicated that the pre-deformation could prolong the duration of the primary creep stage and considerably facilitated the creep strain.

Spigarelli and Sandstrom [25] presented basic creep modelling of the pure aluminum, which was compared to experimental data. Lei et al. [26] investigated thermal-mechanical loading sequences related creep ageing behaviors of the 7050 aluminum alloy. They showed that the alternative of the ageing furnace or the autoclave could cause inverse thermal-mechanical loading sequences, including loading prior to heating in the ageing furnace or heating prior to loading in the autoclave. El Amri et al. [27] performed thermal and also thermo-mechanical simulations in the 6061 aluminum alloy. They applied a numerical procedure to assess the thermo-mechanical damage at high temperatures, using the ABAQUS software. They depicted that the performance of the proposed model was good. Belodedenko et al. [28] studied fatigue resistance models of structures for the risk-based inspection. They proposed two basic models, including the lifetime general equation and the lifetime dispersion equation.

Consequently, in the mentioned literature review, all articles were about creep behaviors of aluminum alloys. However, in the following, more details of another literature review could be seen for aluminum matrix composites whose articles are rare in comparison to those of aluminum alloys.

Cadek et al. [29] studied the threshold creep behavior of discontinuous aluminum and aluminum alloy matrix composites. They showed that the creep-strengthening effect of silicon carbide particulates, silicon carbide whiskers and alumina short fibers was high, although particulates, whiskers and short fibers did not represent effective obstacles to dislocation motions. Ji et al. [30] investigated the creep behavior of TiC<sub>p</sub>/2618 aluminum matrix composite at 250, 300 and 350°C. Their results indicated that both the stress exponent and the apparent activation energy of the composite were higher than those of the 2618 aluminum alloy. They depicted that the existence of TiC particles significantly improved the high-temperature creep property of the 2618 aluminum alloy. On this research, Gonzalez-Doncel and Fernandez [31] presented some comments. They improved the creep response of 2618Al with 15 and 20 vol.% of TiC<sub>p</sub>, assuming a mechanism of the load transfer from the aluminum alloy matrix to TiC<sub>p</sub>. Fernandez and Gonzalez-Doncel [32] checked the creep fracture behavior of aluminum alloys and aluminum alloy metal matrix composites. They found a good correlation between

experimental data and results of the phenomenological Monkman-Grant model.

Choi and Bae [33] investigated creep properties (at 250°C) of aluminum-based composites, containing 4.5 vol.% of multi-walled carbon nanotubes (CNT). They depicted that the composite had higher creep resistance at the applied stress, higher than 200 MPa. Below 110 MPa, the composite showed a negligible dependency of the strain rate on the stress, due to the diffusional flow of the matrix, which was significantly restricted by nanotubes. Sudharshan Phani and Oliver [34] performed a comparison of high-temperature nano-indentation creep and uniaxial creep measurements 27-550°C for the commercial purity aluminum. Uniaxial power-law creep parameters (the stress exponent and the pre-exponential term) were calculated from indentation data, for the comparison of results to uniaxial data. Their results demonstrated a good agreement with literature values. Saberi Kakhki et al. [35] studied impression relaxation behaviors of Al/4%-SiC nano-composites. They showed a constant relation between the stress relaxation and the compression creep rate. SiC nano-particles acted as work-hardening areas, the porosity and the non-symmetrical distribution of SiC caused variations of the steady state relaxation rate or creep rate. Zhao et al. [36] improved elevated-temperature mechanical properties of Al-Mn-Mg, containing TiC nano-particles. They indicated that TiC nano-particles significantly increased the strength at the ambient temperature and at 200°C. At higher temperatures, such strengthening effect diminished, due to the activated dislocation climb.

As a conclusion on the second part of the literature review, it could be concluded that several articles were published on creep properties of aluminum alloys. Moreover, creep properties of the nano-composite were rarely published. Different nano-particles were introduced such as CNT [33], SiC [35], TiC [37], Al<sub>2</sub>O<sub>3</sub> and CuO [38], with the weight percentage of 1-4% [35,38]. In addition, creep behaviors of piston aluminum-silicon alloys, with and without SiO<sub>2</sub> nano-particles, as a special case study, were experimentally studied in this research. This could be the novelty, since no report could be found on such a material. Besides, this article has been presented to complete previous researches [1-3]. It should be noted that in the literature [38], 2% SiO<sub>2</sub> nano-particles were added to the aluminum alloy, which led to lower creep properties. In this report, the weight percentage of nano-particles reduced to 1% and creep experiments were done under different temperatures. For this objective, standard test samples were casted, machined and tested under creep loading under a constants load. Then, obtained results are presented in figures and tables. Therefore, the structure of this article includes the introduction, experimental works, results, the discussion and conclusions.

## 2. EXPERIMENTAL WORKS

In this article, the studied material was a piston aluminum alloy. The chemical composition of this material was 12.5 wt.% Si, 0.4 wt.% Fe, 2.4 wt.% Cu, 0.7 wt.% Mg and 2.2 wt.% Ni, besides the aluminum matrix. The flowchart for the whole stages of experimental works in this research is shown in Figure 1.

To reinforce the material, SiO<sub>2</sub> nano-particles were used to add into the aluminum matrix. Azadi and Aroo [38] reported that 2% SiO<sub>2</sub> nano-particles reduced the creep lifetime of the material. Therefore, in this research, the weight percentage was considered as 1%. For this objective, nano-particles were firstly coated by aluminum micro-powders in a planetary ball mill device. More details of such works were presented in the literature [1-3]. As an important note and based on previous reports [1-3], the X-ray diffraction (XRD) analysis and images of the transmission electron microscopy (TEM) showed a proper process for coating.

The fabrication technique for the piston aluminum-silicon alloy was the gravity casting approach. The production method for the aluminum matrix nano-composite was the stir-casting process. Cylindrical specimens were initially casted in a cast-iron permanent mold for aluminum-silicon alloys, unreinforced and reinforced by nano-particles. After casting, nano-composite specimens were also heat treated at 500°C for 5 h, quenched in water and aged at 180°C for 9 h [39]. More details for fabricating samples could be seen in the literature [38].

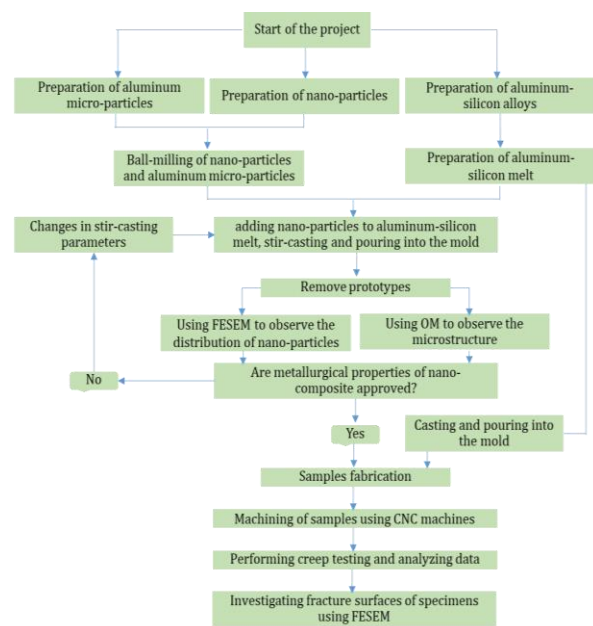


**Figure 1.** The flowchart of experimental works in this research.

For the experimental investigation, creep tests were carried out on the studied material, based on the ASTM-E139-11 standard [40]. The applied stress was 100 MPa in all creep tests on both materials. This loading case was considered due to working conditions of engine pistons [38]. However, the temperature was considered as 250, 275 and 300°C. Since the maximum temperature of pistons in internal combustion engines has been around 300°C [10, 16]. The creep specimen geometry is depicted in Figure 2. Dimensions are in millimeter in Figure 2. Standard specimens were machined from casted cylinders, made from the aluminum-silicon alloy and the aluminum alloy nano-composite. Creep tests were performed by the SCT-300 creep testing machine (SANTAM Company). More descriptions of tests could be observed in the literature [41].

To study the fracture surface, the field-emission scanning electron microscopy (FE-SEM) was used based on the MIRA TESCAN model, in the secondary mode. In addition, the energy dispersive X-ray spectroscopy (EDS) map was utilized to indicate the chemical composition of materials, in the back-scattered mode of FE-SEM images. In addition, the other objective of the back-scattered FE-SEM image was to check the distribution of nano-particles in the matrix. Then also, to find the effect of the heat treatment and nano-particles, before testing, microstructures were examined by the optical microscopy (OM), using the Olympus model. For such objective, a polishing process was firstly performed on specimens and then, a Keller etchant was used [1,3].

### 3. RESULTS and DISCUSSION

As a first result, the microstructure of aluminum-silicon alloys, unreinforced and reinforced with nano-particles, before creep testing, can be seen in Figure 3, including OM images. It should be noted that the nano-composite was also heat treated, as mentioned. According to Figure 3, both materials had almost the same microstructure, based on observed phases. However, the size of different phases was not the same in the aluminum-silicon alloy, with and without nano-particles.

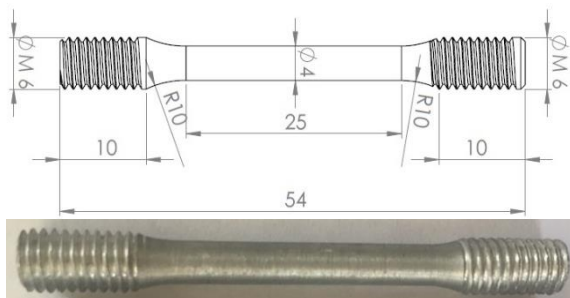


**Figure 2.** The specimen geometry in millimeter of creep testing, based on the ASTM-E139-11 standard

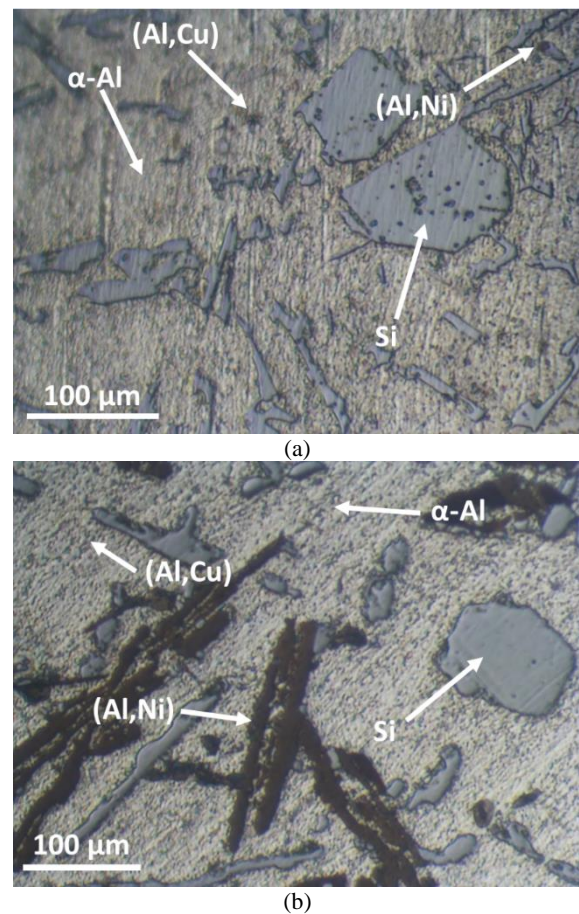


**Figure 3.** Microstructures of aluminum alloys, (a) unreinforced and (b) reinforced with nano-particles, before creep testing.

The investigated material had different phases [1,3]. The first phase was the matrix ( $\alpha$ -Al) whose color was light gray. The second phase was Si, which was homogeneously distributed in the matrix in a blocky form, including polyhedral crystals with a flaky morphology. Zainon et al. [42] reported that there were two types of Si phase, including the flake-like form and the coarse primary Si particle. The intermetallic phase was (Al,Ni), which could be seen in a black-colored regime. Another intermetallic phase was (Al,Cu) with a brown color. Such obtained results are consistent with those reported in the literature [43-45].

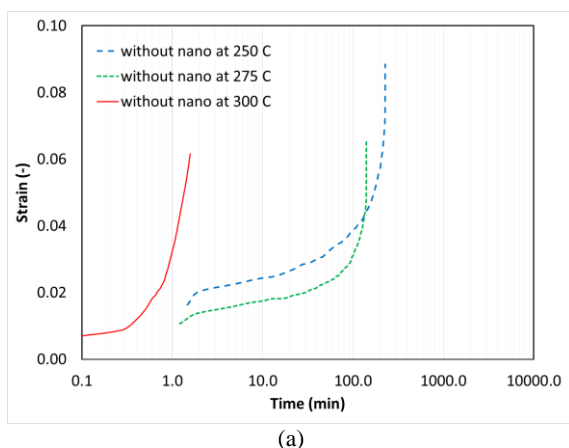
The heat treatment increased the amount of the (Al,Ni) intermetallic phase in the aluminum matrix. Such phenomenon could enhance and improve the strength of the material. In addition, the shape of the Si phase, after the heat treatment, became the flake-like morphology. Then also, adding SiO<sub>2</sub> nano-particles to the aluminum matrix caused to change the morphology of the (Al,Ni) intermetallic phase, into the flaky shape. Besides, nano-particles were joined to the Si phase and therefore, higher amount of Si could be seen in the microstructure of the

nano-composite. However, the size of the Si phase decreased by nano-particles. As a result, the ratio of the diameter to the length for intermetallic phases and the Si phase decreased. Such presented results were reported in the literature [45-46]. In addition, Issa et al. [47] found a decrease in the grain size, when ceramic nano-particles reinforced the matrix.

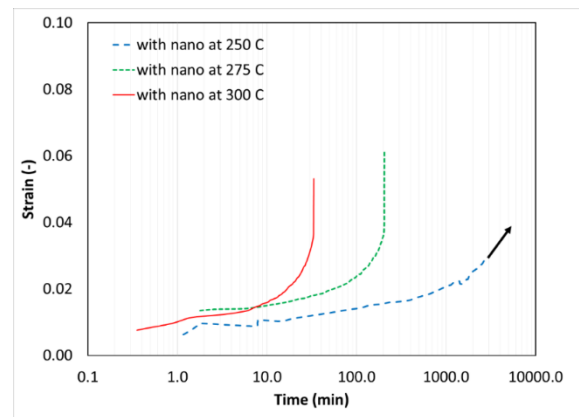
Besides OM images, in order to illustrate the distribution of nano-particles in the aluminum matrix, the back-scattered FE-SEM image was also checked. More details about this investigation could be found in the literature [1,3]. As a result, based on the reported results in previous works [48-49], the maximum size of nano-particles in the matrix was less than 100 nm, which showed no agglomeration. Besides, the distribution of nano-particles in the aluminum matrix was also proper.

Obtained results from creep testing, including curves of the strain versus the time and the strain rate versus the time can be seen in Figures 4 and 5. It should be noted that a logarithmic scale was used for the time and the strain rate, to show all data in a wide range. As another note, one creep test was stopped for the nano-composite at 250°C, due to limitation of facilities. This long creep time was more than 46.8 h, which is equal to about 2 days of testing. As another note, for data at 300°C, curves of the strain and also the strain rate were logically differentiated from curves for two other temperatures.

Besides creep curves, Table 1 shows creep results, including the minimum strain rate, the rupture strain and the rupture time. Based on these results, as expected, by increasing the temperature, the creep lifetime of materials decreased. This creep lifetime of the nano-composite improved 1135 (at least), 46 and 1988%, when compared to the creep lifetime of the aluminum-silicon alloy, at 250, 275 and 300°C, respectively. The second value (46%) for such improvement at 275°C of the material by

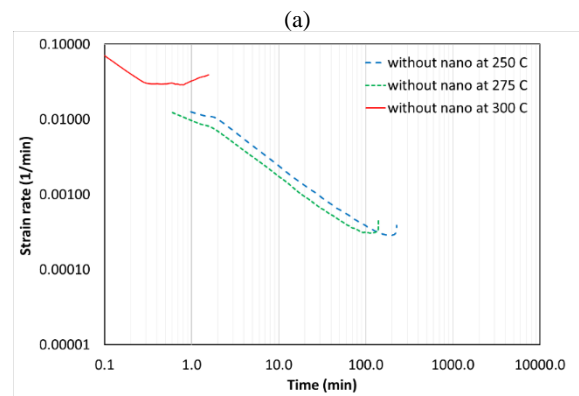


(a)

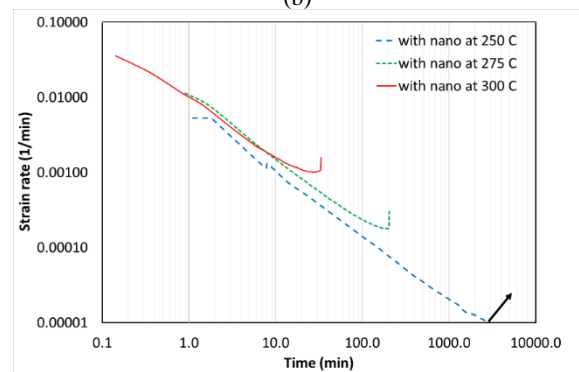


(b)

**Figure 4.** The strain versus the time for aluminum alloys, (a) unreinforced and (b) reinforced with nano-particles



(a)



(b)

**Figure 5.** The strain rate versus time for aluminum alloys, (a) unreinforced and (b) reinforced with nano-particles

adding SiO<sub>2</sub> nano-particles was not in the order of other enhancement values. It means that the sample could have higher creep lifetime. The reason was to have a big microstructural defect due to the casting process. However, the creep lifetime of the nano-composite was still higher than that of the aluminum alloy, without nano-particles. This claim could be proved by FE-SEM images of the fracture surface as follows.

**TABLE 1.** Results of creep testing on aluminum alloys, unreinforced and reinforced with nano-particles

Temperature (°C)	Minimum strain rate (1/min)	Rupture strain (-)	Rupture time (min)
<b>Without nano-particles</b>			
250	0.000286	0.0885	227.3
275	0.000306	0.0658	140.1
300	0.028907	0.0616	1.6
<b>With nano-particles</b>			
250	Not finished	Not finished	>2807.1
275	0.000179 Diff.: 42%	0.0618 Diff.: 6%	205.1 Diff.: 46%
300	0.001014 Diff.: 96%	0.0531 Diff.: 14%	33.4 Diff.: 1988%

\*Diff.: Percentage difference comparing to data without nano-particles.

The rupture strain decreased, when the temperature enhanced, for both aluminum-silicon alloys, unreinforced and reinforced one with nano-particles. The rupture strain for the nano-composite was lower than the rupture strain of the aluminum-silicon alloy, at all temperatures. Besides, by increasing the temperature, the minimum strain rate increased. This minimum strain rate decreased when nano-particles were added to the aluminum alloy, without nano-particles. Such results were also represented in the literature [6,12], for aluminum alloys. Ishikawa and Kobayashi [6] indicated that the minimum strain rate had the dependence to the applied stress and the temperature. Besides, increasing the temperature caused to the enhancement of the minimum strain rate. Such same results were observed in the research. Kandarea et al. [12] showed that by increasing the temperature, the creep lifetime decreased, which showed a good agreement with the obtained results of this article.

To find the activation energy ( $Q$ ) for the creep behavior in aluminum-silicon alloys, unreinforced and reinforced with nano-particles, the following equation could be used [50]:

$$\dot{\epsilon}_{min} = A \exp\left(\frac{-Q}{RT}\right) \quad (1)$$

in which,  $\dot{\epsilon}_{min}$  is the minimum strain rate,  $A$  is a material constant,  $R$  is the gas global constant, which is 8.314 J/mol.K and  $T$  is the temperature in Kelvin. By using a logarithmic scale for such equation and curve fitting, one obtains:

$$\ln(\dot{\epsilon}_{min}) = \ln(A) - \left(\frac{Q}{R}\right) \frac{1}{T} \quad (2)$$

And comparing to a linear equation, such as  $Y = \bar{Y} - \bar{X}X$ , where:

$$Y = \ln(\dot{\epsilon}_{min}), \bar{Y} = \ln(A), \bar{X} = \frac{Q}{R}, X = \frac{1}{T} \quad (3)$$

the material constant and the activation energy could be found. Obtained results for such investigation is shown in Figure 6.

The coefficient of determination for the aluminum-silicon alloy, without nano-particles, was about 74%, according to the mentioned problem for the sample at 300°C (having a sudden failure and very low creep lifetime and high minimum strain rate). For the nano-composite, there were only two data, since the creep test at 250°C was not finished. However, it was over-predicted in Figure 6. Therefore, no proper conclusion could be generally obtained from these results, since there was a non-proper variation in experimental data. In further investigations, the repeatability of testing would be performed for a proper conclusion. However, the number of experimental data was enough for comparing results of aluminum alloys, with and without nano-particles. Thus, it could be claimed that reported experimental data was reliable.

However, based on obtained results in Figure 6, the activation energy was calculated as 181.2 and 226.6 kJ/mol, for aluminum-silicon alloys, unreinforced and reinforced with nano-particles, respectively. Consequently, the addition of nano-particles into the matrix reduced the activation energy of the material. However, this statement could not be correct due to the non-proper variation in testing. In other words, this range of activation energy (181.2-226.6 kJ/mol) was due to the low repeatability of testing and it seems that nano-particles have no significant effect on the activation energy. The only claim for such values is that the range of the obtained activation energy for aluminum alloys was in agreement with presented values (in the range of 142-249 kJ/mol) in the literature [6-8, 27-30, 34]. Ji et al. [30] represented the activation energy for aluminum matrix composites in the range of 226-272 kJ/mol.

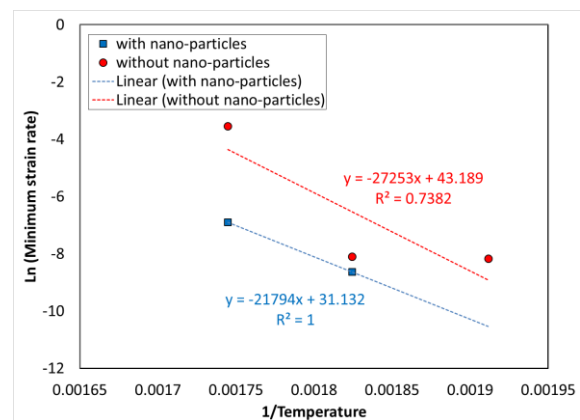


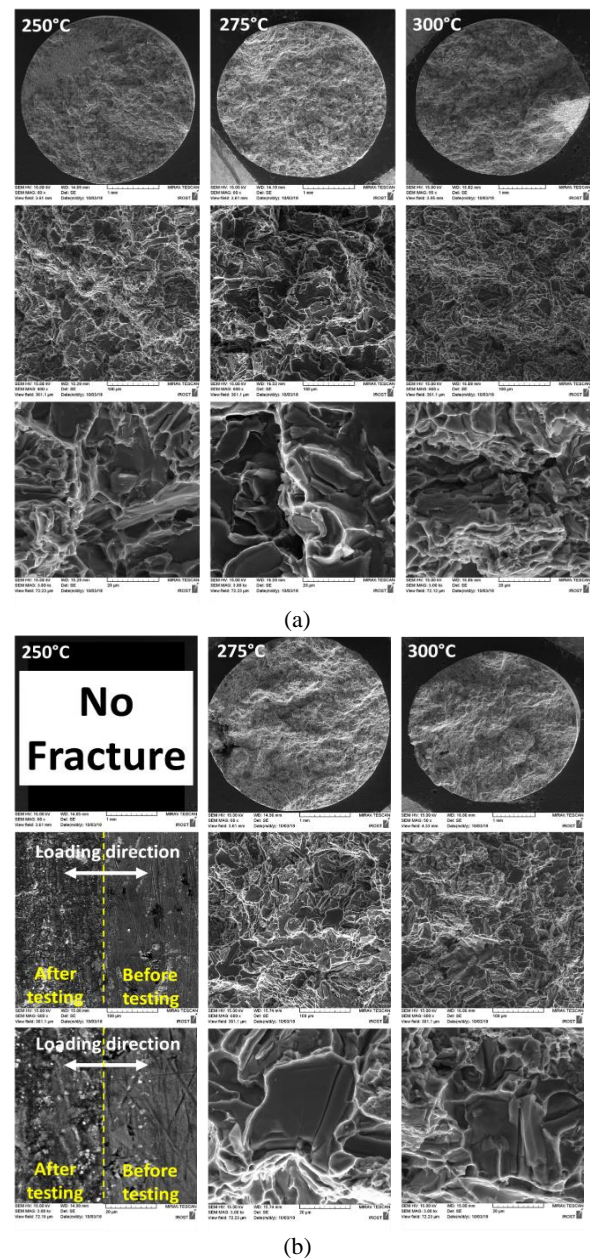
**Figure 6.** The curve for  $\ln(\dot{\epsilon}_{min})$  versus  $\frac{1}{T}$  for aluminum alloys, unreinforced and reinforced with nano-particles

Besides the activation energy, the material constant,  $A$ , for the nano-composite had lower value ( $3.3 \times 10^{13}$ ), comparing to that of the aluminum-silicon alloy ( $5.7 \times 10^{18}$ ). Therefore, the nano-composite had lower minimum strain rate and higher creep lifetime.

FE-SEM images in different magnifications for aluminum-silicon alloys, unreinforced and reinforced with nano-particle, after creep tests is depicted in Figure 7, to check failure mechanisms based on fracture surfaces. Based on this figure, both materials had a brittle fracture behavior, according to the observed quasi-cleavage marks on all fracture surfaces. In addition, micro-cracks could be seen on quasi-cleavage planes. Such marks were reported by Wang et al. [46,51] for the piston aluminum alloy, under cyclic loadings at 120-425°C. They indicated that at 280°C, brittle quasi-cleavage fractures of the aluminum matrix, with broken silicon platelets and other intermetallic particles, were observed at fracture surfaces. At 350°C, the fracture surface morphology was same as that of 280°C, with some dimples, as a ductile fracture mark. However, at 425°C, the fractography of aluminum alloys changed to a typical ductile fracture with micro-dimples and broken silicon platelets [46]. In other words, increasing the temperature caused to change in fracture characteristics, from brittle to ductile fractures. Such behavior showed that the temperature had a significant effect on mechanical properties and fracture behaviors of aluminum-silicon alloys. It should be noted that fracture surfaces of the aluminum-silicon sample at 300°C had a sudden rupture, since the creep lifetime was 1.6 (min). Therefore, there was no clear cleavage planes and no plastic deformation induced. As another result, the cleavages plane seemed to be bigger for the nano-composite. Bigger cleavage areas and less tear ridges showed the poor ductility [49]. In the literature [46], such results, including lower elongations for the nano-composite, were obtained.

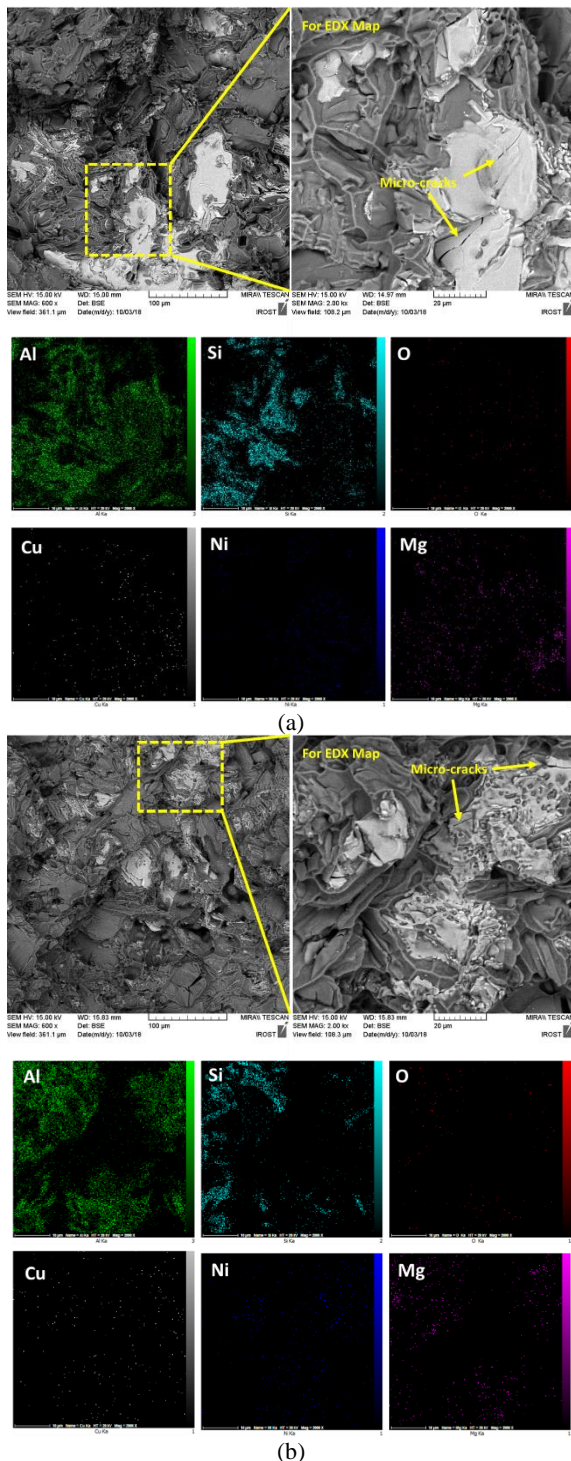
Two important notes for Figure 7(b) are about the sample with nano-particles and low improvement of the creep lifetime at 275°C. For the first note, the standard sample at 250°C was not broken, since the creep test was stopped after about two days. As the second note, it should be mentioned that at 250°C, since there was no fracture, the crept surface of the cylindrical specimen could be compared to the initial sample surface, before testing. After creep testing, the roughness of the specimen surface increased, according to the plastic deformation. For the third note, lower improvement of the creep lifetime at 275°C was due to a big microstructural defect (on the left-hand side of the fracture surface), as mentioned before. Although the sample could experience higher creep lifetime than 205.1 min.

Figure 8 shows back-scattered FE-SEM images with EDX maps for aluminum-silicon alloys, unreinforced



**Figure 7.** The FE-SEM images of fracture surfaces for aluminum alloys, (a) unreinforced and (b) reinforced with nano-particles

and reinforced with nano-particles, after creep testing at 275°C under 100 MPa. As can be seen in Figure 8, the gray-colored regime included Al and Si elements and the white-colored regime included the Ni element, which showed the (Al,Ni) intermetallic phase. As a note, the distribution of other elements had no meaning, in both materials. Based on the EDX map, micro-cracks were observed more inside the intermetallic phase, in the aluminum alloy, without nano-particles. However, in the nano-composite, such micro-cracks were observed at boundaries of the intermetallic phase.



**Figure 8.** The back-scattered FE-SEM image with the EDX map for aluminum alloys, (a) unreinforced and (b) reinforced with nano-particles, after creep tests at 275°C under 100 MPa.

It seems that the failure mechanism improved, when nano-particles were added to the aluminum matrix. The crack path changed from inside the intermetallic phase

into boundaries between (Al,Ni) intermetallic and Si phases. Therefore, the creep lifetime increased for the nano-composite. The crack length in the nano-composite was less than the crack length in the aluminum-silicon alloy, without nano-particles.

Zolfaghari et al. [49] reported that in aluminum-silicon alloys, the failure could be initiated by cleavage marks from intermetallic or Si phases. They added nano-particles in the aluminum matrix to decrease the size of Si phases in the matrix and therefore, increased the fatigue lifetime of the nano-composite. At this condition, Al/Si interface debonding occurred as the failure mechanism, due to the weak interfacial strength. Then, adding nano-particles would increase the strength of the Al/Si interface in the nanocomposite [49].

As another failure mechanism, they also implied that intermetallic phases had significant influences on brittle fractures of aluminum-silicon alloys [49,52]. Rezaeezhad et al. [52] presented that the dispersed distribution of tiny intermetallic phases would increase mechanical properties of aluminum-silicon alloys. After Si particles, the second phase, which had higher phase percentage in the microstructure, was related to the (Al,Ni) intermetallic phase [52]. The third phase in the matrix was the (Al,Cu) intermetallic phase [52]. They claimed that lower content of the (Al,Ni) intermetallic phase could enhance the fatigue lifetime. In this case, the crack nucleated usually from large intermetallic phases. Then, these cracks encountered intermetallic phases and they might progress along intermetallic phases [52]. Therefore, lower amount of the (Al,Ni) intermetallic phase caused higher lifetime.

#### 4. CONCLUSIONS

In the present article, the temperature influence on creep and fracture behaviors of the aluminum matrix nano-composite was investigated and then, compared to those of the AlSi12Cu3Ni2MgFe aluminum-silicon alloy. Experimental data can be described as follows,

- The effect of the temperature on the creep lifetime of materials was significant. There was a decreasing trend for the creep lifetime by increasing the temperature. Besides, by increasing the temperature, the minimum strain rate increased.
- The improvement of the creep lifetime by the addition of SiO<sub>2</sub> nano-particles to the matrix was severely significant. Besides, the minimum strain rate for the nano-composite was lower than the minimum strain rate of the aluminum alloy.
- FE-SEM images of the fracture surface indicated a brittle fracture behavior, based on quasi-cleavage marks, for aluminum alloys, unreinforced and reinforced with nano-particles. However, the cleavages plane was bigger for the nano-composite.



- Back-scattered FE-SEM images with EDX maps showed more micro-cracks inside the intermetallic phase, in the aluminum alloy. However, in the nano-composite, the failure location changed to boundaries of the intermetallic phase.

## 5. ACKNOWLEDGEMENT

Authors thank Motorsazi Pooya Neyestanak (MPN) Company, located in Isfahan, Iran for their financial supports.

## 6. REFERENCES

1. Azadi, M., Safarloo, S., Loghman, F., Rasouli, R., "Microstructural and thermal properties of piston aluminum alloy reinforced by nano-particles", *AIP Conference Proceedings*, Vol. 1920, (2018), 020027. DOI: <https://doi.org/10.1063/1.5018959>
2. Azadi, M., Zolfaghari, M., Rezanezhad, S., Azadi, M., "Preparation of various aluminum matrix composites reinforcing by nanoparticles with different dispersion methods", Proceedings of Iran International Aluminum Conference, Iran, (2018).
3. Azadi, M., Zolfaghari, M., Rezanezhad, S., Azadi, M., "Effects of SiO<sub>2</sub> nano-particles on tribological and mechanical properties of aluminum matrix composites by different dispersion methods", *Applied Physics A*, Vol. 124, No. 5, (2018), 377. DOI: <https://doi.org/10.1007/s00339-018-1797-9>
4. Ishikawa, K., Okuda, H., Kobayashi, Y., "Creep behaviors of highly pure aluminum at lower temperatures", *Materials Science and Engineering A*, Vol. 234-236, (1997), 154-156. DOI: [https://doi.org/10.1016/S0921-5093\(97\)00204-9](https://doi.org/10.1016/S0921-5093(97)00204-9)
5. Jenabali Jahromi, S.A., "Creep behavior of spray-cast 7XXX aluminum alloy", *Materials and Design*, Vol. 23, (2002), 169-172. DOI: [https://doi.org/10.1016/S0261-3069\(01\)00065-6](https://doi.org/10.1016/S0261-3069(01)00065-6)
6. Ishikawa, K., Kobayashi, Y., "Creep and rupture behavior of a commercial aluminum-magnesium alloy A5083 at constant applied stress", *Materials Science and Engineering A*, Vol. 387-389, (2004), 613-617. DOI: <https://doi.org/10.1016/j.msea.2004.01.099>
7. Dobes, F., Milicka, K., "Comparison of thermally activated overcoming of barriers in creep of aluminum and its solid solutions", *Materials Science and Engineering A*, Vol. 387-389, (2004), 595-598. DOI: <https://doi.org/10.1016/j.msea.2004.02.095>
8. Srivastava, V., Williams, J.P., McNee, K.R., Greenwood, G.W., Jones, H., "Low stress creep behavior of 7075 high strength aluminum alloy", *Materials Science and Engineering A*, Vol. 382, (2004), 50-56. DOI: <https://doi.org/10.1016/j.msea.2004.04.047>
9. Lina, J., Kowalewskib, Z.L., Caoa, J., "Creep rupture of copper and aluminum alloy under combined loadings - Experiments and their various descriptions", *International Journal of Mechanical Sciences*, Vol. 47, (2005), 1038-1058. DOI: <https://doi.org/10.1016/j.ijmecsci.2005.02.010>
10. Requena, G., Degischer, H.P., "Creep behavior of unreinforced and short fiber reinforced AlSi12CuMgNi piston alloy", *Materials Science and Engineering A*, Vol. 420, (2006), 265-275. DOI: <https://doi.org/10.1016/j.msea.2006.01.024>
11. Coureau, O., Dunand, D.C., "Creep of aluminum syntactic foams", *Materials Science and Engineering A*, Vol. 488, (2008), 573-579. DOI: <https://doi.org/10.1016/j.msea.2008.01.022>
12. Kandare, E., Feih, S., Kootsookos, A., Mathys, Z., Lattimer, B.Y., Mouritz, A.P., "Creep-based life prediction modelling of aluminum in fire", *Materials Science and Engineering A*, Vol. 527, (2010), 1185-1193. DOI: <https://doi.org/10.1016/j.msea.2009.10.010>
13. Li, L.T., Lin, Y.C., Zhou, H.M., Jiang, Y.Q., "Modeling the high-temperature creep behaviors of 7075 and 2124 aluminum alloys by continuum damage mechanics model", *Computational Materials Science*, Vol. 73, (2013), 72-78. DOI: <https://doi.org/10.1016/j.commatsci.2013.02.022>
14. Maximov, J.T., Duncheva, G.V., Anchev, A.P., Ichkova, M.D., "Modeling of strain hardening and creep behavior of 2024T3 aluminum alloy at room and high temperatures", *Computational Materials Science*, Vol. 83, (2014), 381-393. DOI: <http://dx.doi.org/10.1016/j.commatsci.2013.11.057>
15. Zhan, L.H., Li, Y.G., Huang, M.H., "Effects of process parameters on mechanical properties and microstructures of creep aged 2124 aluminum alloy", *Transactions of Nonferrous Metals Society of China*, Vol. 24, (2014), 2232-2238. DOI: [https://doi.org/10.1016/S1003-6326\(14\)63338-0](https://doi.org/10.1016/S1003-6326(14)63338-0)
16. Fernandez-Gutierrez, R., Requena, G.C., "The effect of spheroidisation heat treatment on the creep resistance of a cast AlSi12CuMgNi piston alloy", *Materials Science and Engineering A*, Vol. 598, (2014), 147-153. DOI: <http://dx.doi.org/10.1016/j.msea.2013.12.093>
17. Zhang, Q., Zhang, W., Liu, Y., "Evaluation and mathematical modeling of asymmetric tensile and compressive creep in aluminum alloy ZL109", *Materials Science and Engineering A*, Vol. 628, (2015), 340-349. DOI: <http://dx.doi.org/10.1016/j.msea.2015.01.032>
18. Spence, T.W., Makhlof, M.M., "The effect of machining-induced residual stresses on the creep characteristics of aluminum alloys", *Materials Science and Engineering A*, Vol. 630, (2015), 125-130. DOI: <http://dx.doi.org/10.1016/j.msea.2015.02.020>
19. Yang, Y.L., Zhan, L.H., Li, J., "Constitutive modeling and spring-back simulation for 2524 aluminum alloy in creep age forming", *Transactions of Nonferrous Metals Society of China*, Vol. 25, (2015), 3048-3055. DOI: [https://doi.org/10.1016/S1003-6326\(15\)63932-2](https://doi.org/10.1016/S1003-6326(15)63932-2)
20. Lei, C., Yang, H., Li, H., Shi, N., Zhan, L.H., "Dependences of microstructures and properties on initial tempers of creep aged 7050 aluminum alloy", *Journal of Materials Processing Technology*, Vol. 239, (2016), 125-132. DOI: <https://doi.org/10.1016/j.jmatprotec.2016.07.004>
21. Erdeniz, D., Nasim, W., Malik, J., Yost, A.R., Park, S., Luca, A.D., Vo, N.Q., Karaman, I., Mansoor, B., Seidman, D.N., Dunand, D.C., "Effect of vanadium micro-alloying on the microstructural evolution and creep behavior of Al-Er-Sc-Zr-Si alloys", *Acta Materialia*, Vol. 124, (2017), 501-512. DOI: <http://dx.doi.org/10.1016/j.actamat.2016.11.033>
22. Xu, Y., Zhan, L., Li, W., "Effect of pre-strain on creep aging behavior of 2524 aluminum alloy", *Journal of Alloys and Compounds*, Vol. 691, (2017), 564-571. DOI: <http://dx.doi.org/10.1016/j.jallcom.2016.08.291>
23. Li, Y., Shi, Z., Lin, J., Yang, Y.L., Rong, Q., "Extended application of a unified creep-ageing constitutive model to multistep heat treatment of aluminum alloys", *Materials and Design*, Vol. 122, (2017), 422-432. DOI: <http://dx.doi.org/10.1016/j.matdes.2017.03.023>
24. Yang, Y., Zhan, L., Shen, R., Yin, X., Li, X., Li, W., Huang, M., He, D., "Effect of pre-deformation on creep age forming of 2219 aluminum alloy: Experimental and constitutive modelling",

- Materials Science and Engineering A*, Vol. 683, (2017), 227-235. DOI: <http://dx.doi.org/10.1016/j.msea.2016.12.024>
25. Spigarelli, S., Sandstrom, R., "Basic creep modelling of aluminum", *Materials Science and Engineering A*, Vol. 711, (2018), 343-349. DOI: <https://doi.org/10.1016/j.msea.2017.11.053>
  26. Lei, C., Li, H., Zheng, G.W., Fu, J., "Thermal-mechanical loading sequences related creep aging behaviors of 7050 aluminum alloy", *Journal of Alloys and Compounds*, Vol. 731, (2018), 90-99. DOI: <https://doi.org/10.1016/j.jallcom.2017.10.035>
  27. Cadek, J., Oikawa, H., Gustek, V., "Threshold creep behavior of discontinuous aluminum and aluminum alloy matrix composites: An overview", *Materials Science and Engineering A*, Vol. 190, (1995), 9-23. DOI: [https://doi.org/10.1016/0921-5093\(94\)09605-V](https://doi.org/10.1016/0921-5093(94)09605-V)
  28. El Amri, A., El Haddou, M., Khamlichi, A., "Thermal-mechanical coupled manufacturing simulation in heterogeneous materials", *Civil Engineering Journal*, Vol. 2, No. 11, (2016), 600-606. DOI: [10.28991/cej-2016-00000062](https://doi.org/10.28991/cej-2016-00000062)
  29. Belodedenko, S., Hanush, V., Baglay, A., Hrechanyi, O., "Fatigue resistance models of structural for risk based inspection", *Civil Engineering Journal*, Vol. 6, No. 2, (2020), 375-383. DOI: [10.28991/cej-2020-03091477](https://doi.org/10.28991/cej-2020-03091477)
  30. Ji, F., Ma, M.Z., Song, A.J., Zhang, W.G., Zong, H.T., Liang, S.X., Osamu, Y., Liu, R.P., "Creep behavior of in situ TiC<sub>p</sub>/2618 aluminum matrix composite", *Materials Science and Engineering A*, Vol. 506, (2009), 58-62. DOI: <https://doi.org/10.1016/j.msea.2008.11.010>
  31. Gonzalez-Doncel, G., Fernandez, R., "Comments on "Creep behavior of in situ TiC<sub>p</sub>/2618 aluminum matrix composite"", *Materials Science and Engineering A*, Vol. 527, (2010), 3288-3292. DOI: <https://doi.org/10.1016/j.msea.2008.11.010>
  32. Fernandez, R., Gonzalez-Doncel, G., "Understanding the creep fracture behavior of aluminum alloys and aluminum alloy metal matrix composites", *Materials Science and Engineering A*, Vol. 528, (2011), 8218-8225. DOI: <https://doi.org/10.1016/j.msea.2011.07.027>
  33. Choi, H.J., Bae, D.H., "Creep properties of aluminum-based composite containing multi-walled carbon nanotubes", *Scripta Materialia*, Vol. 65, (2011), 194-197. DOI: <https://doi.org/10.1016/j.scriptamat.2011.03.038>
  34. Sudharshan Phani, P., Oliver, W.C., "A direct comparison of high temperature nano-indentation creep and uniaxial creep measurements for commercial purity aluminum", *Acta Materialia*, Vol. 111, (2016), 31-38. DOI: <http://dx.doi.org/10.1016/j.actamat.2016.03.032>
  35. Saberi Kakhki, Y., Nategh, S., Mirdamadi, T.S., "Impression relaxation and creep behavior of Al/SiC nano-composite", *Materials and Technology*, Vol. 50, No. 4, (2016), 611-615. DOI: [10.17222/mit.2015.113](https://doi.org/10.17222/mit.2015.113)
  36. Zhao, Q., Zhang, H., Zhang, X., Qiu, F., Jiang, Q., "Enhanced elevated-temperature mechanical properties of Al-Mn-Mg containing TiC nano-particles by pre-strain and concurrent precipitation", *Materials Science and Engineering A*, Vol. 718, (2018), 305-310. DOI: <https://doi.org/10.1016/j.msea.2018.01.123>
  37. Barzegar, M.H., Fallahiyekta, M., "Increasing the thermal efficiency of double tube heat exchangers by using nano hybrid", *Emerging Science Journal*, Vol. 2, No. 1, (2018), 11-19. DOI: <http://dx.doi.org/10.28991/esj-2018-01122>
  38. Azadi, M., Aroo, H., "Creep properties and failure mechanisms of aluminum alloy and aluminum matrix silicon oxide nano-composite under working conditions in engine pistons", *Materials Research Express*, Vol. 6, No. 11, (2019), 115020. DOI: <https://doi.org/10.1088/2053-1591/ab455f>
  39. Zeren, M., "The effect of heat-treatment on aluminum-based piston alloys", *Materials and Design*, Vol. 28, (2007), 2511-2517. DOI: <https://doi.org/10.1016/j.matdes.2006.09.010>
  40. Standard test methods for conducting creep, creep-rupture and stress-rupture tests of metallic materials, ASTM-E1391, ASTM International, (2012).
  41. Azadi, M., Azadi, M., "Evaluation of high-temperature creep behavior in Inconel-713C nickel-based superalloy considering effects of stress levels", *Materials Science and Engineering A*, Vol. 689, (2017), 298-305. DOI: <https://doi.org/10.1016/j.msea.2017.02.066>
  42. Zainon, F., Rafezi Ahmad, K., Daud, R., "Effect of heat treatment on microstructure, hardness and wear of aluminum alloy 332", *Applied Mechanics and Materials*, Vol. 786, (2015), 18-22. DOI: <https://doi.org/10.4028/www.scientific.net/AMM.786.18>
  43. Han, L., Sui, Y., Wang, Q., Wang, K., Jiang, Y., "Effects of Nd on microstructure and mechanical properties of cast Al-Si-Cu-Ni-Mg piston alloys", *Journal of Alloys and Compounds*, Vol. 695, (2017), 1566-1572. DOI: <https://doi.org/10.1016/j.jallcom.2016.10.300>
  44. Humbertjean, A., Beck, T., "Effect of the casting process on microstructure and lifetime of the Al-piston-alloy AlSi12Cu4Ni3 under thermo-mechanical fatigue with superimposed high-cycle fatigue loading", *International Journal of Fatigue*, Vol. 53, (2013), 67-74. DOI: <https://doi.org/10.1016/j.ijfatigue.2011.09.017>
  45. Mollaei, M., Azadi, M., Tavakoli, H., "A parametric study on mechanical properties of aluminum-silicon/SiO<sub>2</sub> nano-composites by a solid-liquid phase processing", *Applied Physics A*, Vol. 124, (2018), 504. DOI: <https://doi.org/10.1007/s00339-018-1929-2>
  46. Wang, M., Pang, J.C., Li, S.X., Zhang, Z.F., "Low-cycle fatigue properties and life prediction of Al-Si piston alloy at elevated temperature", *Materials Science and Engineering A*, Vol. 704, (2017), 480-492. DOI: <https://doi.org/10.1016/j.msea.2017.08.014>
  47. Issa, H.K., Taherizadeh, A., Maleki, A., Ghaei, A., "Development of an aluminum/amorphous nano-SiO<sub>2</sub> composite using powder metallurgy and hot extrusion processes", *Ceramics International*, Vol. 43, (2017), 14582-14592. DOI: <https://doi.org/10.1016/j.ceramint.2017.06.057>
  48. Rezaezhad, S., "Investigation of heat treatment effect on bending high-cycle fatigue properties in aluminum-silicon alloy, with and without nano-particles", MSc Thesis, Semnan University, Iran, (2018).
  49. Zolfaghari, M., Azadi, M., Azadi, M., "Characterization of high-cycle bending fatigue behaviors for piston aluminum matrix SiO<sub>2</sub> nano-composites in comparison with aluminum-silicon alloys", *International Journal of Metalcasting*, (2020), DOI: <https://doi.org/10.1007/s40962-020-00437-y>
  50. Bahmanabadi, H., Rezaezhad, S., Azadi, M., Azadi, M., "Characterization of creep damage and lifetime in Inconel-713C nickel-based superalloy by stress-based, strain/strain rate-based and continuum damage mechanics models", *Materials Research Express*, Vol. 5, No. 2, (2018), 026509. DOI: <https://doi.org/10.1088/2053-1591/aaab04>
  51. Wang, M., Pang, J.C., Zhang, M.X., Liu, H.Q., Li, S.X., Zhang, Z.F., "Thermo-mechanical fatigue behavior and life prediction of the Al-Si piston alloy", *Materials Science and Engineering A*, Vol. 715, (2018), 62-72. DOI: <https://doi.org/10.1016/j.msea.2017.12.099>
  52. Rezaezhad, S., Azadi, M., Azadi, M., "Influence of heat treatment on high-cycle fatigue and fracture behaviors of piston aluminum alloy under fully-reversed cyclic bending", *Metals and Materials International*, (2019), DOI: <https://doi.org/10.1007/s12540-019-00498-7>

---

**Persian Abstract**

---

**چکیده**

در این مقاله، تاثیر دما بر خواص خزشی و رفتار شکست آلیاژ  $AlSi12Cu3Ni2MgFe$  آلومینیوم-سیلیسیوم، تقویت نشده و تقویت شده با ذرات نانو، مورد بررسی قرار گرفت. برای این منظور، نمونه‌های استاندارد به روش ریخته‌گری تغلی و ریخته‌گری گردابی، به ترتیب برای آلیاژ آلومینیوم و نانوکامپوزیت، ساخته شدند. آزمون خزش نیرو-کنترل، بر روی نمونه‌های استاندارد در سطوح دمایی ۲۵۰، ۲۷۵ و ۳۰۰ درجه سانتیگراد و سطح تنش ۱۰۰ مگاپاسکال انجام شد. سپس، برای شناسایی مکانیزم‌های خرابی، سطح شکست نمونه‌های آزمون با میکروسکوپ الکترون روبشی نشر میدانی، مورد مطالعه قرار گرفت. نتایج تجربی نشان داد که دما، بصورت موثری، رفتار خزش هر دو ماده را تغییر می‌دهد. بعلاوه، با افزودن ذرات نانو و عملیات حرارتی به ماتریس آلومینیوم، بهبود قابل توجهی در خواص خزشی مشاهده شد. چنین افزایشی در عمر خزشی، در دمای ۳۰۰ درجه سانتیگراد بیشتر بود. همچنین، بررسی سطح شکست هر دو ماده نشان داد که رفتار شکست بصورت ترد با آثار شبه‌کلویچ بود. در نمونه‌های نانوکامپوزیتی، موقعیت شکست از داخل فازهای بین‌فلزی به مرزهای فازهای بین‌فلزی تغییر کرد.

---